Supplementary Information (SI) for Green Chemistry.

Supporting Information

Catalyst-Free Urea Synthesis via Plasma-Driven Direct Coupling of CO_2 and N_2 under Ambient Conditions

Dingwei Gan[a], Jingwen Huang[a], Longfei Hong[a], Haoxuan Jiang[a], Xiaoran Wang[a], Rusen Zhou[a], Jing Sun[a], and Renwu Zhou*[a]

a State Key Laboratory of Electrical Insulation and Power Equipment, Centre for Plasma Biomedicine, School of Electrical Engineering, Xi'an JiaoTong University, Xi'an 710049, China.

** The corresponding Author:*

Prof. Renwu Zhou

Email：renwu.zhou@xjtu.edu.cn

This supporting information contains the following sections:

1. Experiment methods

A plasma power supply (Leap100, PlasmaLeap Technologies, Sydney, Australia), capable of providing a high voltage pulse up to 80 kV (p–p), a repetitive pulse frequency from 100 to 3000 Hz, and maximum output power of 400 W. The power supply parameters are set at discharge: resonance frequency – 60 kHz; discharge frequency - 1500 Hz; duty cycle- 100 μS; input voltage - 150 V. The voltage and current waveforms of the discharge were measured using a high-voltage probe (Tektronix P6015A) and a current probe (Person 2877), combined with a digital oscilloscope (Tektronix MDO3054). Plasma treatment was conducted for a duration of 10 minutes. The discharge reactor consisted of a 150 mL double-layer glass beaker containing 100 mL of ultrapure water as the treatment medium. In the single-bubble reactor (SR) configuration, the plasma bubble generator was positioned at the center of the beaker's bottom. In contrast, the dual-bubble reactor (DR) configuration employed two bubble generators symmetrically placed on opposite sides of the beaker to ensure spatial separation of the discharge zones.

Plasma bubble reactors were fabricated using quartz tubes with an inner and outer diameter of 5.0 and 8.0 mm, respectively. Different numbers of laser-drilled microholes (1, 4 and 8 holes, 500 μm in diameter) were uniformly distributed around the base of the outer quartz tube to allow atmospheric CO_2 and N_2 (1.0 L min^{-1} in total) to flow through the tube and diffuse into the aqueous solution. In SR, the position of the bubble reactor is at the middle bottom of the beaker. In DR, the bubble reactors are located on both sides of the beaker.

A digital oscilloscope (RIGOL DS6104) was employed to record the applied voltage and current with a high voltage probe (Tektronics P6015A) and a current probe (Pearson 4100), respectively. The discharge power was calculated based on our previously reported studies[1]. A spectrometer (Andor Shamrock SR-500i-A-R) was used to obtain the optical emission spectra (OES) of the discharges, reactive species in the gas phase plasma and to validate the formation of the secondary chemical species. The spectrometer was equipped with CCD detector.

The energy efficiency calculation formula. In the equation, T represents the duration of a discharge period, u and i represent the plasma voltage and current within a discharge period. V represents the volume of the treated solution.

$$\text{Urea Formation rate } (\text{mmol} \cdot h^{-1}) = \frac{\text{Concentration of } urea \text{ (mmol/L)} \times V\,(L)}{\text{discharge time } (h)}$$

$$P_{\text{discharge}} = \frac{1}{T}\int_0^T u(t)i(t)dt$$

$$\eta_{urea}\left(\text{mmol} \cdot (\text{kW} \cdot h)^{-1}\right) = \frac{urea \text{ produced } (\text{mmol} \cdot h^{-1})}{P_{\text{discharge}}\,(\text{kW})}$$

The pH, ORP and conductivity of PAW were measured immediately after plasma discharge using a pH detector with a temperature sensor, a redox meter and an electric conductivity detector, respectively (SANXIN SX620, 630 and 650).

LC-MS were performed on Thermo Scientific Q-Exactive Plus system in positive mode. The MS instrument parameters were as follows: spray voltage of 3800 V, sheath gas flow rate of 3 L• min-1, capillary temperature at 320 °C. Mass spectra were registered in the scan range from m/z=50 to 750. The HPLC was performed on UltiMate 3000 HPLC system and fitted with a Phenomenex Luna 5um C18(2) 100A LC Column 250*4.6mm. The column temperature was maintained at room temperature. The HPLC flow rate was 1 mL• min^{-1}.

The following chromatographic procedures were used.

Chromatographic procedures	Solvent A	Solvent B
0-4 min, 5% B; 4-19 min, 5-70% B; 19-21 min, 70% B; 21-22 min, 70-5% B; 22-30 min, 5%B	0.1 % FA + 99.9 % H_2O	ACN

Samples were dissolved in a phosphate buffer (pH 2.5) in D_2O and ^1H NMR spectra were recorded using Bruker 600 MHz spec-trometer and TopSpin, with a temperature of 298 K, a t1 relaxation delay of 15 s, and collecting of 64 scans. The ^{13}C NMR spectra were recorded using Bruker

600 MHz spectrometer and TopSpin, with a temperature of 298 K and collecting of 256 scans. All spectra were processed and plotted using the Mest ReNova Software.

Formic acid is confirmed and quantified by ion chromatography (IC) and the H is measured using the spin trap agent DMPO by an electron spin resonance (ESR) spectrometer (Bruker, EMXplus).

2. Discharge waveform

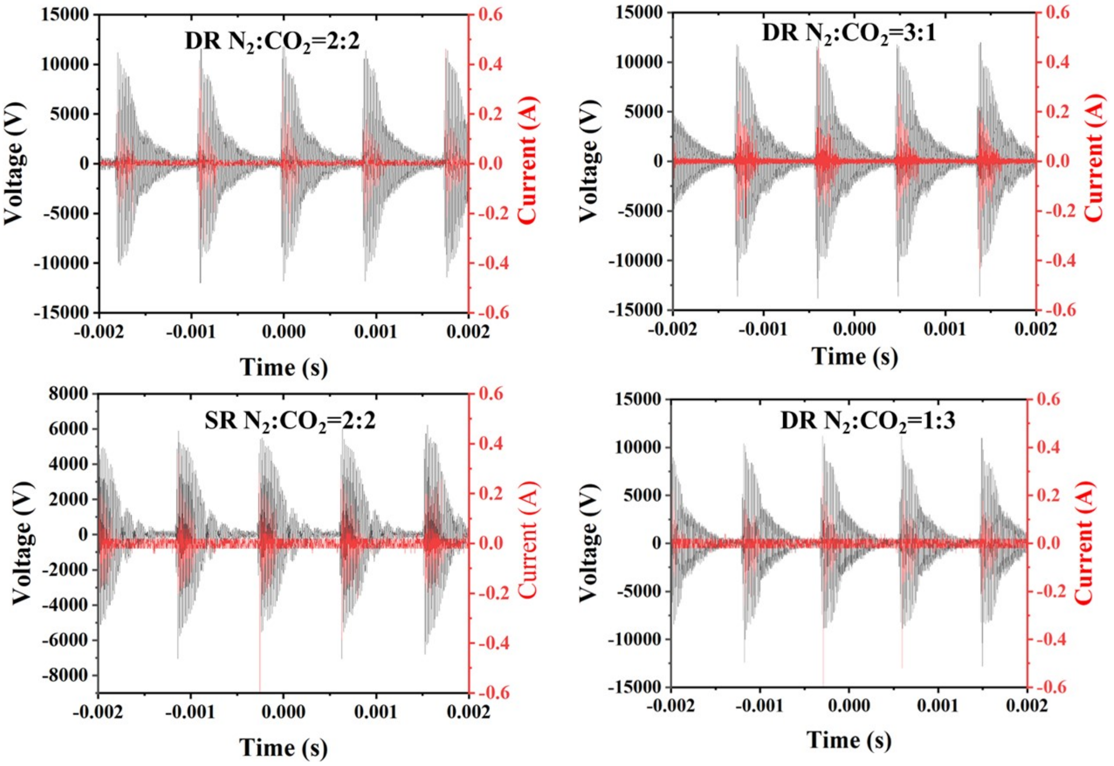

Fig. S1 Discharge waveform in different gas ratio (N_2/CO_2).

3. Discharge plasma platform

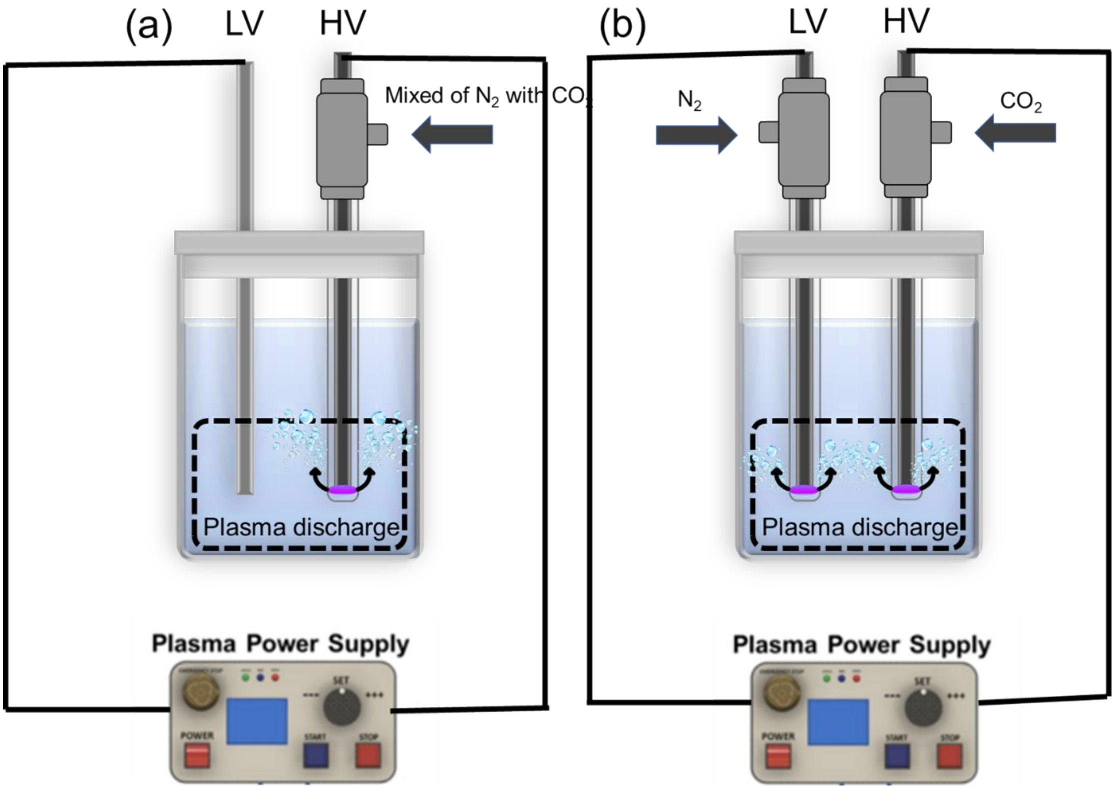

Fig. S2 Discharge plasma platform.

4. Standard curve

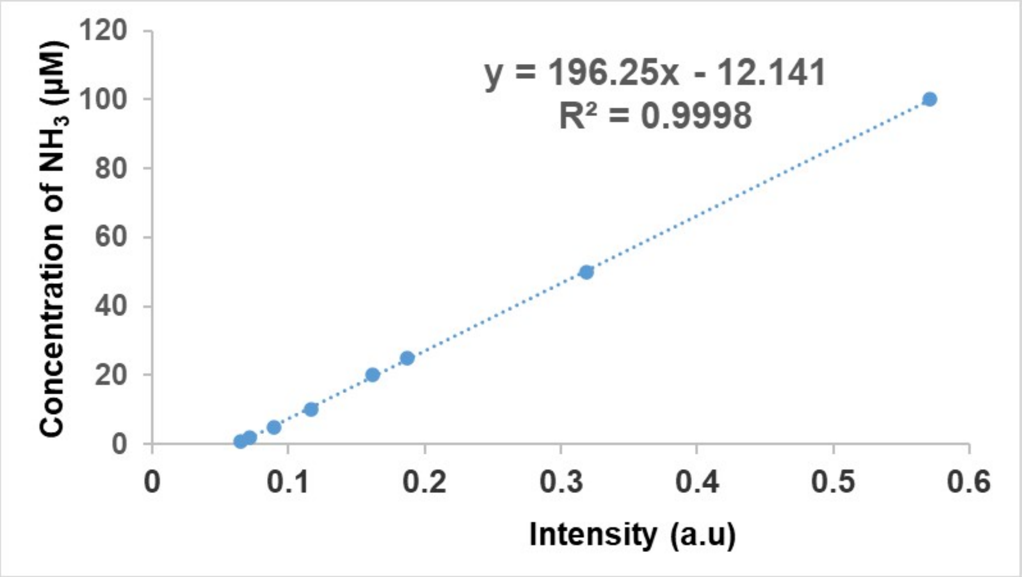

Fig. S3 Standard curve of NH_3.

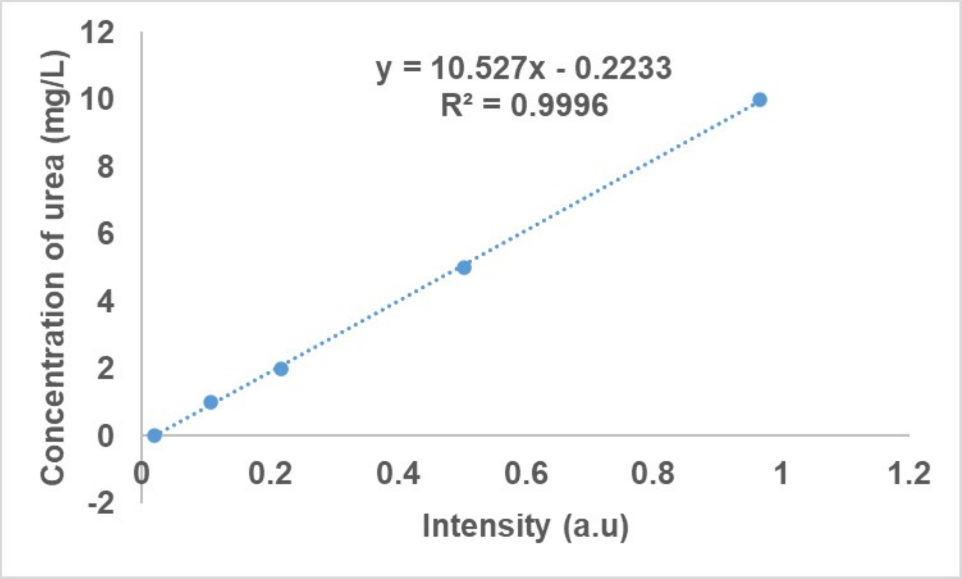

Fig. S4 Standard curve of urea.

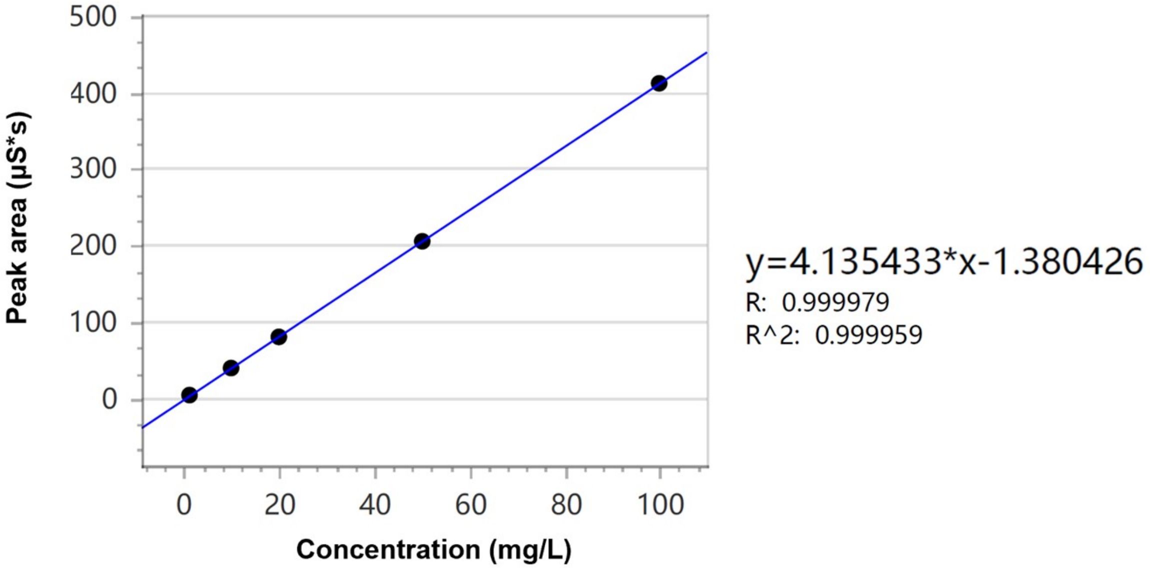

Fig. S5 Standard curve of HCOOH.

The principle of NO_3^- detection is to convert NO_3^- to NO_2^-, measure the total nitrogen concentration, and subtract the NO_2^- concentration. The standard curve of NO_2^- and the total nitrogen concentration (NO_2^- +NO_3^-) are shown in Fig. S6.

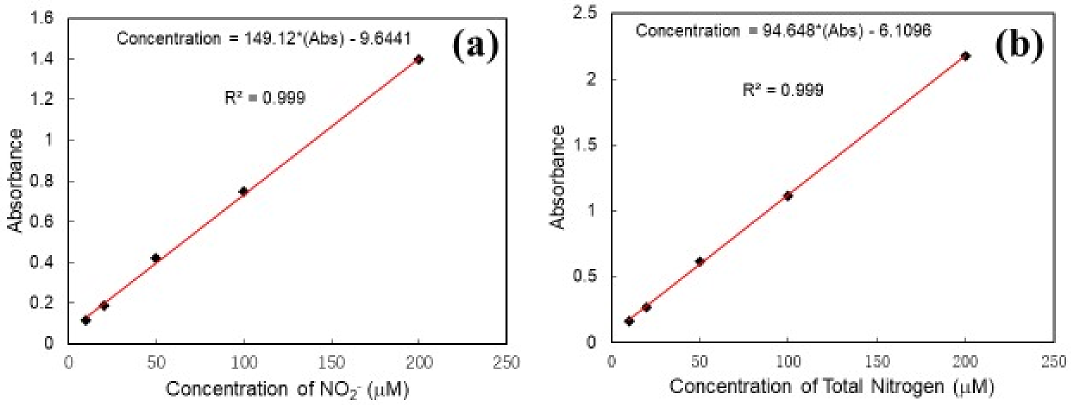

Fig. S6 The standard curve of (a) NO_2^- and (b) total nitrogen concentration

5. Other supporting profiles

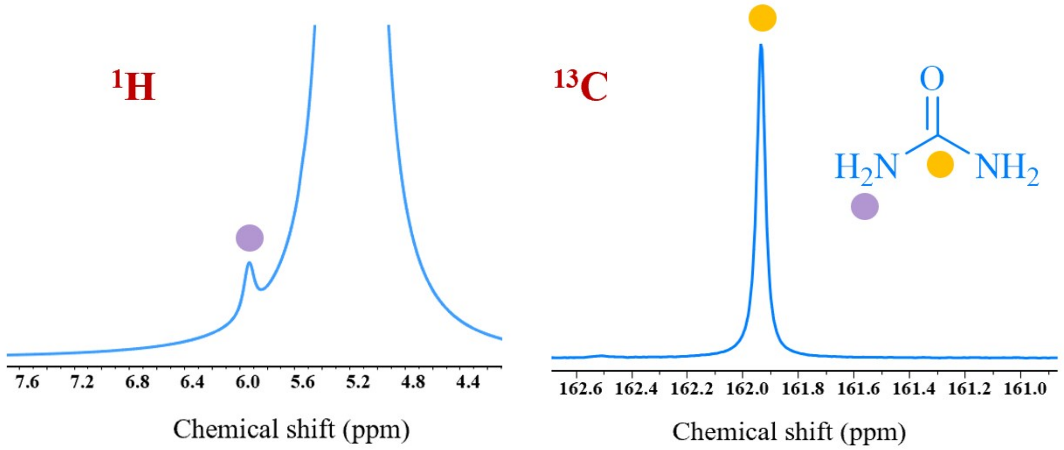

Fig. S7 NMR profile of sample, which confirmed the formation of urea.

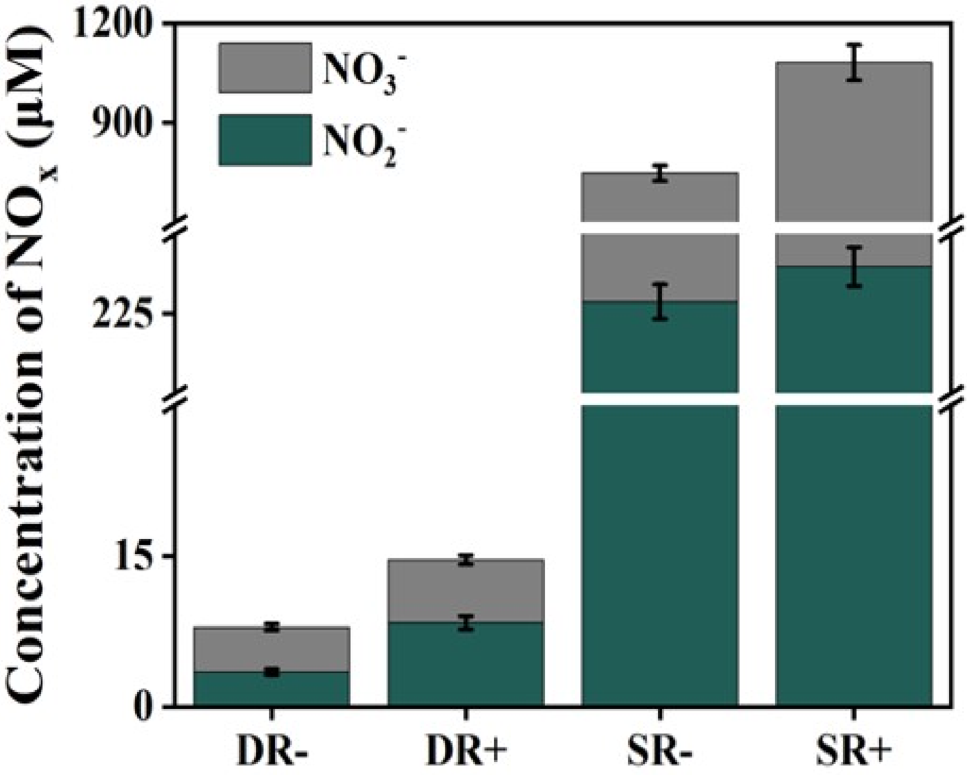

Fig. S8 Concentration of NOx formed in both DR and SR. (+: adding Mannitol; -: without Mannitol)

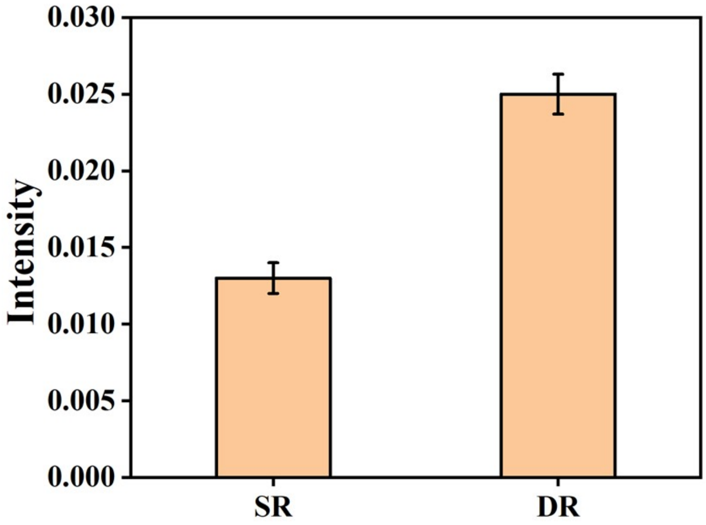

Fig. S9 The Intensity (peak intensity) of H radical.

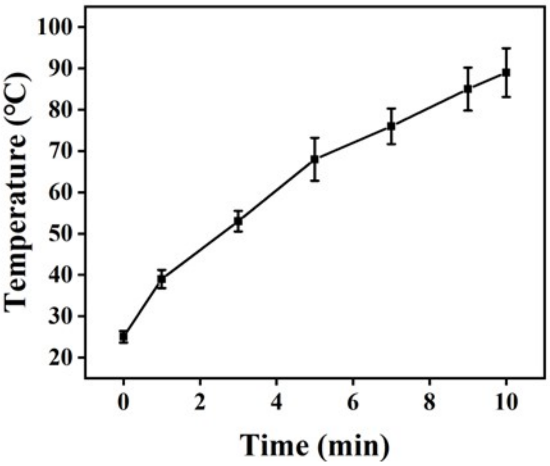

Fig. S10 Plasma-induced temperature changes (N_2: CO_2=3:1, DR).

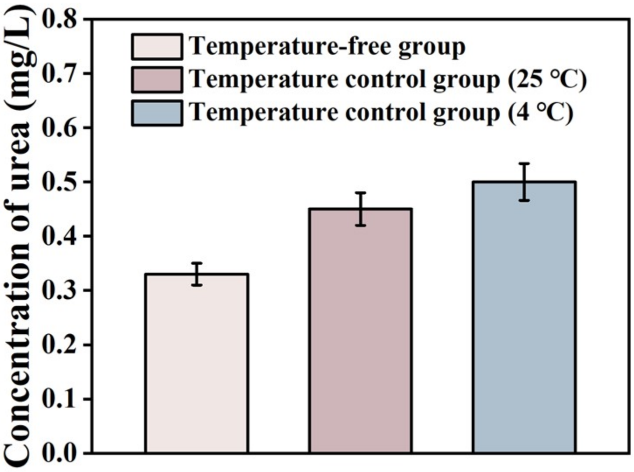

Fig. S11 The influence of temperature on urea yield (N_2: CO_2=3:1, DR).

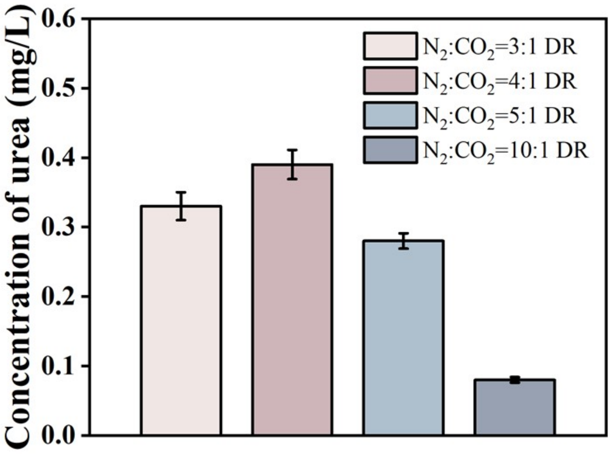

Fig. S12 The influence of gas ratio of N_2/CO_2 on urea yield.

Comparison between the plasma process and the traditional catalytic system

It is acknowledged that the energy efficiency of the present plasma-based approach is lower than that of catalytic processes, particularly electrocatalysis, which benefits from inherently low power consumption and can achieve high energy efficiency under mild conditions. However, in terms of product yield, this work offers a notable advantage. The urea production rate reaches up to 0.5 mg/h, which surpasses most previously reported non-catalytic methods and is competitive with many catalytic systems, placing it in the upper-middle range of reported yields. Although the energy efficiency remains a limitation, the overall process—ranging from feedstock selection to operational conditions—strictly adheres to the principles of green and sustainable chemistry. The method avoids hazardous reagents, operates under ambient conditions, and offers a catalyst-free route, making it a viable and environmentally benign strategy for distributed or modular urea synthesis.

Table S1. The comparison between the plasma process and the traditional catalytic system.

Cathode/ Catalyst	Energy Efficiency (mg/kWh)	Urea Yield (mg/h)	FE (%)	Current Density (mA/cm2)	Applied potential (V vs. RHE)	Ref.
Bi-$BiVO_4$	88738.65	0.32	12.55	3	-0.4	2
In In-OH	308558.25	0.37	20.97	1	-0.4	3
$BiFeO_3$/$BiVO_4$	13486.2	0.27	17.18	16.5	-0.4	4
Pd_1Cu_1/TiO_2-400	201801.6	0.04	8.92	0.5	-0.4	5
$Ni_3(BO_3)_2$-150	233032.8	0.52	20.36	1.5	-0.5	6

ZnMn−N,Cl	800800	0.05	28.7	0.2	-0.3	7
Bi_2S_3/N-RGO	462462	0.18	7.5	0.8	-0.5	8
ZIF-8	701415	0.09	22.03	1.25	−0.1	9
$Sb_xBi_{1-x}O_y$	/	0.03	10.9	/	-0.3	10
/	**2**	**0.1**	/	/	/	**11**
/	**6**	**0.2**	/	/	/	**This work**

Table S2 Comparison between plasma process and photocatalysis systems for urea synthesis

Cathode/ Catalyst	Urea Yield (mg/h)	Apparent Quantum Yield (%)	Wavelength (nm)	Ref.
CeO_2-500	0.0155	/	/	12
None	**0.3**	**/**	**/**	**This work**

Table S3. The selectivity of N was calculated here:

Product	Selectivity of N in DR	Selectivity of N in SR
NO_3^-	8 μM (5%)	747 μM (67%)
NO_2^-	4 μM (2.5%)	236 μM (23.7%)
NH_3	140 μM (88.4%)	30 μM (3%)
Urea	6.6 μM (4.1%)	3.2 μM (0.3%)

As the table showed, the DR shows better urea selectivity than SR.

Reference

1. C. Man, C. Zhang, H. Fang, R. Zhou, B. Huang, Y. Xu, X. Zhang, T. Shao, Plasma Processes Polym. 2022; 19:e2200004

2. M. Yuan, J. Chen, Y. Bai, Z. Liu, J. Zhang, T. Zhao, Q. Wang, S. Li, H. He and G. Zhang, Unveiling Electrochemical Urea Synthesis by Co-Activation of CO2 and N2 with Mott–Schottky Heterostructure Catalysts, 2021, 60, 10910-10918.

3. M. Yuan, H. Zhang, Y. Xu, R. Liu, R. Wang, T. Zhao, J. Zhang, Z. Liu, H. He, C. Yang, S. Zhang and G. Zhang, Artificial frustrated Lewis pairs facilitating the electrochemical N2 and CO2 conversion to urea, Chem Catalysis, 2022, 2, 309-320.

4. M. Yuan, J. Chen, Y. Bai, Z. Liu, J. Zhang, T. Zhao, Q. Shi, S. Li, X. Wang and G. Zhang, Electrochemical C–N coupling with perovskite hybrids toward efficient urea synthesis, Chemical Science, 2021, 12, 6048-6058.

5. C. Chen, X. Zhu, X. Wen, Y. Zhou, L. Zhou, H. Li, L. Tao, Q. Li, S. Du, T. Liu, D. Yan, C. Xie, Y. Zou, Y. Wang, R. Chen, J. Huo, Y. Li, J. Cheng, H. Su, X. Zhao, W. Cheng, Q. Liu, H. Lin, J. Luo, J. Chen, M. Dong, K. Cheng, C. Li and S. Wang, Coupling N2 and CO2 in H2O to synthesize urea under ambient conditions, Nature Chemistry, 2020, 12, 717-724.

6. M. Yuan, J. Chen, Y. Xu, R. Liu, T. Zhao, J. Zhang, Z. Ren, Z. Liu, C. Streb, H. He, C. Yang, S. Zhang and G. Zhang, Highly selective electroreduction of N2 and CO2 to urea over artificial frustrated Lewis pairs, Energy & Environmental Science, 2021, 14, 6605-6615.

7. X. Zhang, X. Zhu, S. Bo, C. Chen, K. Cheng, J. Zheng, S. Li, X. Tu, W. Chen, C. Xie, X. Wei, D. Wang, Y. Liu, P. Chen, S. P. Jiang, Y. Li, Q. Liu, C. Li and S. Wang, Electrocatalytic Urea Synthesis with 63.5 % Faradaic Efficiency and 100 % N-Selectivity via One-step C−N coupling, 2023, 62, e202305447.

8. P. Xing, S. Wei, Y. Zhang, X. Chen, L. Dai and Y. Wang, Electrochemical Co-reduction of N2 and CO2 to Urea Using Bi2S3 Nanorods Anchored to N-Doped Reduced Graphene Oxide, ACS Applied Materials & Interfaces, 2023, 15, 22101-22111.

9. J. Yuan, Z. Liu, L. Ma, Z. Feng and K. Zhu, Communication—Electrochemical Reduction of CO2 and N2 into Urea at ZIF-8 Cathode, Journal of The Electrochemical Society, 2023, 170, 043503.

10. X. Chen,S. Lv,J. Kang,Z. Wang,T. Guo,Y. Wang,G. Teobaldi,L. Liu,& L. Guo, Efficient C–N coupling in the direct synthesis of urea from CO2 and N2 by amorphous SbxBi1-xOy clusters, Proc. Natl. Acad. Sci. U.S.A. 120 (39) e2306841120

11. Rathore, V., Desai, V., Jamnapara, N.I. and Nema, S.K. (2025), Green Pathway of Urea Synthesis Through Plasma–Ice Interaction: Optimization and Mechanistic Insights With $N_2 + CO_2$ and $NH_3 + CO_2$ Gas Mixtures. Plasma Processes and Polymers, 22: 2400218.

12. S. Yang, W. Zhang, G. Pan, J. Chen, J. Deng, K. Chen, X. Xie, D. Han, M. Dai, L. Niu, Angew. Chem. Int. Ed. 2023, 62, e202312076.